Nanoarray of Polycyclic Aromatic Hydrocarbons and Carbon Nanotubes for Accurate and Predictive Detection in Real-World Environmental Humidity

Yael Zilberman,[†,§] Radu Ionescu,[†,§] Xinliang Feng,[‡] Klaus Müllen,[‡] and Hossam Haick[†,*]

[†]The Department of Chemical Engineering and Russell Berrie Nanotechnology Institute, Technion—Israel Institute of Technology, Haifa 32000, Israel, and [‡]Max-Planck-Institute for Polymer Research, Postfach 3148, D-55021 Mainz, Germany. [§]These authors have contributed eqally to this work.

ABSTRACT In the present work, we introduce a cross-reactive array of synthetically designed polycyclic aromatic hydrocarbons (PAH) and single-walled carbon nanotube (SWCNT) bilayers and demonstrate the huge potential of the array in discriminating between polar and nonpolar volatile organic compounds (VOCs), as well as between the different VOCs from each subgroup. Using appropriate combinations of PAH/SWCNT sensors, we demonstrate that high sensitivity and accuracy values can be obtained for discriminating polar and nonpolar VOCs in samples with variable humidity levels (5—80% RH). The same array of sensors exhibited self-learning capabilities that facilitated exchanging information about environmental properties under observation. The results presented here could lead to the development of a cost-effective, lightweight, low-power, and non-invasive tool for a widespread detection of VOCs in real-world environmental, security, food, health, and other applications.

KEYWORDS: polycyclic aromatic hydrocarbon · carbon nanotube · sensor · nonpolar · polar · humidity

Sensor development is a rapidly evolving field that is driven by the increasing demand for fast online detection of a wide range of chemical and biological species in different branches of industry, homeland security, environmental monitoring, and medicine.[1−7] An emerging sensing strategy that is useful for the analysis of complex mixtures of relatively similar compounds involves the use of arrays of broadly cross-reactive sensors.[1,4,6,8] Sensor arrays mimic the biological systems responsible for the sense of smell and of taste.[4] Every constituent sensor in an array responds to all (or to a large subset) of the mixture compounds.[4,8,9] Logically, the sensors should be sufficiently diverse to provide individually different responses to a given mixture but do not have to be strictly chemically selective.

A wide variety of excellent sensors have been developed for sophisticated sensor array applications (see refs 1, 4−6, 8, and 10−14 and literature therein). Desirable attributes of sensor arrays for important real-world applications, such as quality control or point-of-care diagnosis (*cf.* ref 15) include appropriate detection limits and, at the same time, a wide dynamic range, tolerance for variable chemical backgrounds, room temperature operation, reasonable size and mass, low cost, *etc*. The possibilities to achieve these attributes by fine-tuning sensors that are based on bulk materials, especially for applications in actual confounding humidity conditions, are rather limited. Indeed, real-world applications with gas sensors are hindered by the high and/or not constant humidity levels present in the environment and/or detected sample.

Recent studies have shown that hybrid structures containing a quasi-2D network of single-walled carbon nanotubes (SWCNTs) and organic layers can overcome many of these limitations and, simultaneously, yield devices that are simpler to fabricate.[5,11−13,16,17] A random network of SWCNTs coated with on-chip VOC-amplifiers—for example, films of the non-polar nanographene molecule hexa-*peri*-hexabenzocoronene (HBC)—showed different sensing signals when separately and successively exposed to (either polar or nonpolar) VOCs or water molecules.[18,19] As a typical polycyclic aromatic hydrocarbon (PAH), HBC and its derivatives are particularly interesting for this application because (i) they organize into nano- or microcolumns with distinctive geometrical and morphological features; (ii) they expose only

* Address correspondence to hhossam@technion.ac.il.

Received for review June 22, 2011 and accepted July 20, 2011.

Published online July 20, 2011
10.1021/nn202314k

their side groups to the VOCs; and/or (iii) they hold promise for futuristic sensors that are based on single PAH nano- or microcolumns.[20,21] Additionally, depending on the device configuration, PAH assemblies can be used as an adsorption layer having either semiconducting or relatively insulating properties.[22]

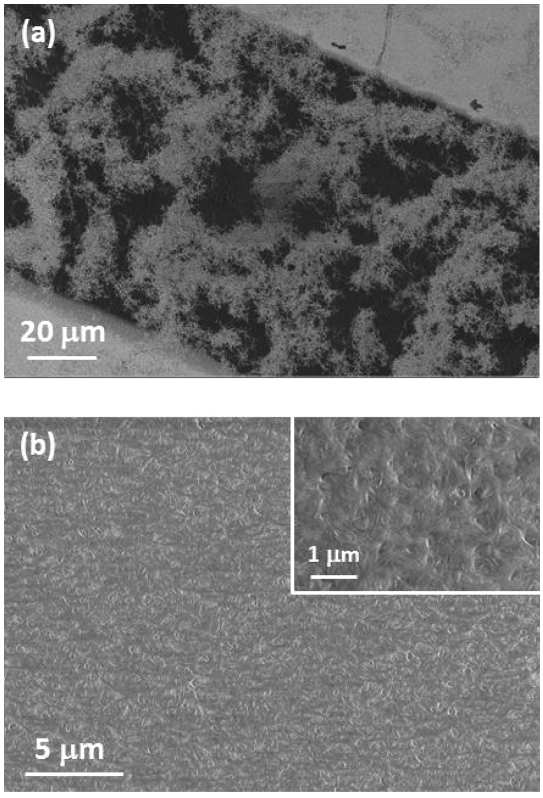

Figure 1. Scanning electron micrograph of (a) SWCNT between two adjacent electrodes in ID configuration; and (b) SWCNT coated with PAH-1 structures.

In this article, we show that an array of cross-reactive PAH and SWCNT bilayers can detect both polar and nonpolar VOCs under various humidity conditions resembling the conditions in real-world applications. Furthermore, we provide evidence that the discriminative power of the sensor array is obtained primarily by controlling the aromatic corona and functional substituents of the PAHs. The results presented here are a major step toward the development of a cost-effective, portable, and non-invasive tool for real-world sensing applications.

RESULTS AND DISCUSSION

The sensors developed in this study were composed from bilayers of PAH derivatives and random network of SWCNTs. A random network of pristine SWCNTs served as a reference sample. Figure 1a shows a typical scanning electron microscopy (SEM) micrograph of a random network of intersecting SWCNTs dispersed between ID electrodes. As seen in the figure, the SWCNTs have made up many paths connecting the two adjacent electrodes together.[17,23] This geometry possesses several advantages: it eliminates conductivity variations due to nanotube chirality and geometry and is tolerant to individual SWCNT channel failure because the device characteristics are averaged over a large number of nanotubes.[1,2] Elimination of alignment and assembly problems[17] is an additional benefit of the random network of SWCNTs; consequently, they can be integrated into devices of arbitrary size using conventional microfabrication technology (*cf.* also ref 24).

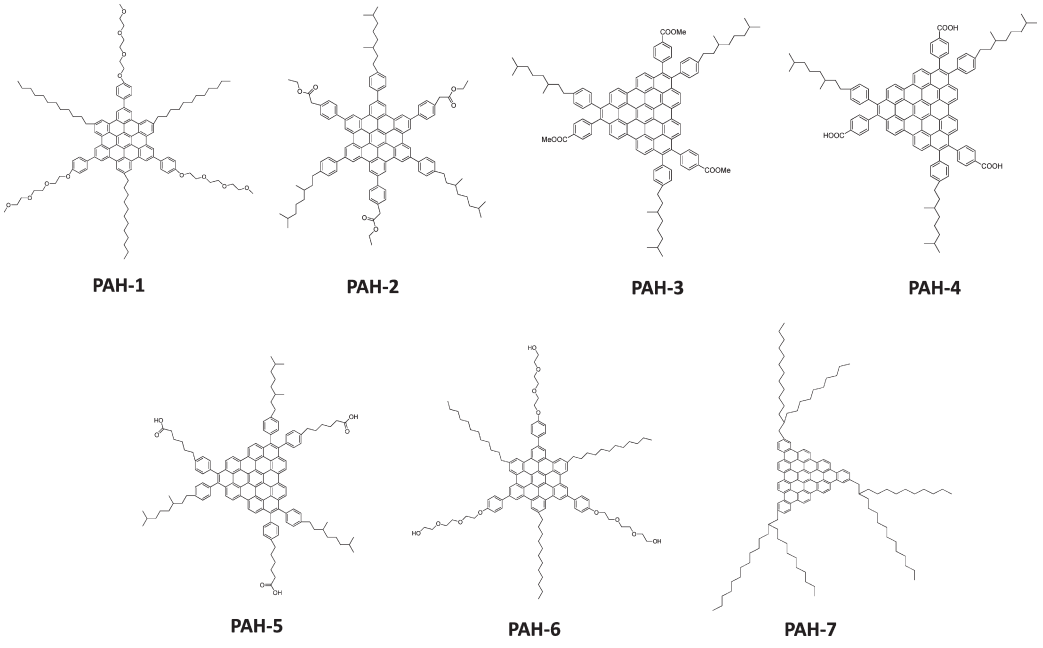

Figure 2. Discotic hexa-*peri*-hexabenzocoronene (PAH) derivatives used in the experiment.

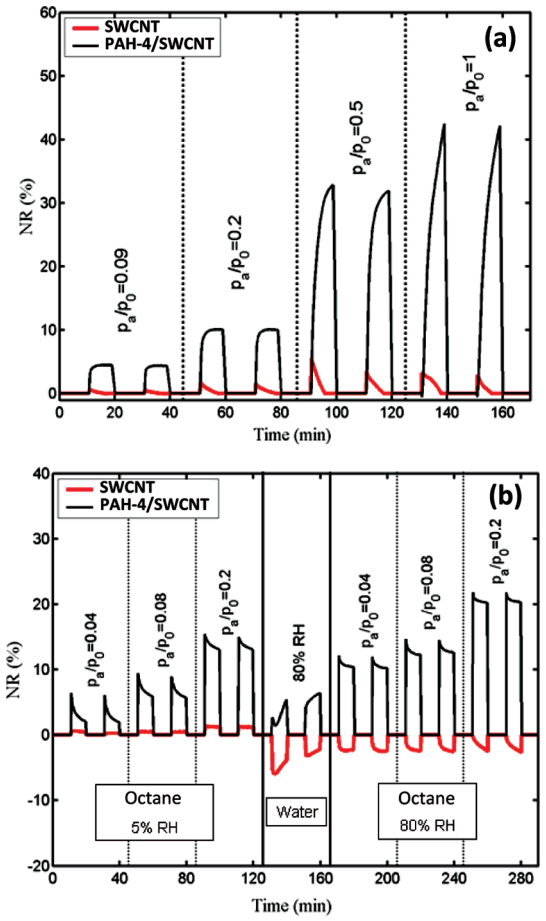

Figure 3. Sensor response to successive concentrations of (a) hexanol diluted in synthetic dry air; (b) octane diluted in both dry (5% RH) and highly humid (80% RH) airflow, and the response to 80% RH. Red curve: response acquired by the pristine SWCNT sensor. Black curve: response acquired by the PAH-4-functionalized SWCNT sensor.

To impart cross-reactive adsorption properties, the SWCNTs were coated with continuous layers (1−2 μm thickness) of PAH derivatives (see Figure 1b). We convincingly demonstrate that employing PAHs with various aromatic corona and functional substituents enables reliable discrimination between different VOCs as well as between different VOCs and various humidity levels (see Methods). Additionally, we show that the same sensors can detect small VOC concentrations from VOC and water mixtures (see Methods).

Figure 3 presents the normalized response, NR (or $\Delta R/R_b$, where R_b is the baseline resistance of the sensor in the absence of analyte and ΔR is the resistance change upon analyte exposure) of a pristine SWCNT and PAH-4/SWCNT sensors (where PAH-4 is a PAH molecule terminated by carboxylic acid groups *via* a phenylene bridge) to successive VOC concentrations (represented by p_a/p_o, where p_a is the partial pressure of the VOC and p_o is the saturated vapor pressure at 21 °C). As seen in Figure 3a, the pristine SWCNTs produced a change in the NR upon exposure to hexanol. Nevertheless, the sensitivity (*i.e.*, the change in the measurement signal per VOC concentration) and reproducibility from cycle to cycle were rather low. Coating the SWCNTs with the PAH-4 layer increased the NR value (at a given concentration) and the sensor sensitivity in a significant manner. For $p_a/p_o = 0.5$ or 1, the S_e (see Methods) calculated from the PAH-4/SWCNT sensor exceeded by 1 order of magnitude the S_e calculated from the pristine SWCNTs. Remarkably, the PAH-4 coating increased the reproducibility of the sensors from cycle to cycle (see Figure 3a) and from sample to sample (not shown). This is an important achievement, as the lack of reproducibility and drift are well-known drawbacks of the gas sensors, mainly those containing SWCNTs. As reference devices, pristine PAH devices (baseline resistance = 1−2 TΩ) exhibited no changes beyond the intrinsic noise upon exposure to the tested analytes and pertinent concentrations (not shown).

Figure 4 presents image plots of the S_e values calculated from the pristine SWCNT and PAH/SWCNT sensors upon successive exposure to various concentrations of VOCs and water molecules. Each point in these plots is an average of two independent exposures from two duplicated sensors.[25] The main observations emerging from these plots follow

(i) The incorporation of the PAH derivatives improved the sensing signals toward part or all of the tested VOCs, compared to pristine SWCNTs.

(ii) The PAH-5/SWCNT provided the highest sensing signals for ethanol, compared to the other PAH derivatives. As an exemplary illustration, the S_e value calculated for ethanol (228.4% at p_a/p_o = 1) was *ca.* 3 times higher than the S_e value calculated for the PAH-4/SWCNT sensor (69.9% at $p_a/p_o = 1$). The high affinity of the PAH-5 to ethanol can readily be attributed to the carboxyl group of the substituent functionality.

(iii) The detection of the OH-terminated (polar) VOCs was most likely promoted by the presence of oxygen in the substituent functionality (*i.e.*, PAH-1, PAH-2, PAH-4, PAH-5, and PAH-6). The longer the OH-terminated VOC, the lower the sensing signal. In light of this correlation, it is likely that the longer the OH-terminated VOC, and the lower the adsorption in the PAH layer, most probably due to an increased steric effect (*cf.* refs 26 and 27).

(iv) All PAH/SWCNTs exhibited high responses upon exposure to ethyl benzene. This can be explained by van der Waals interactions between the benzene rings of the ethyl benzene and PAH corona (which is made of fused benzene rings).[28−30]

(v) The response of the PAH/SWCNTs to water vapor was relatively low, compared to the other VOCs tested under similar p_a/p_o conditions.

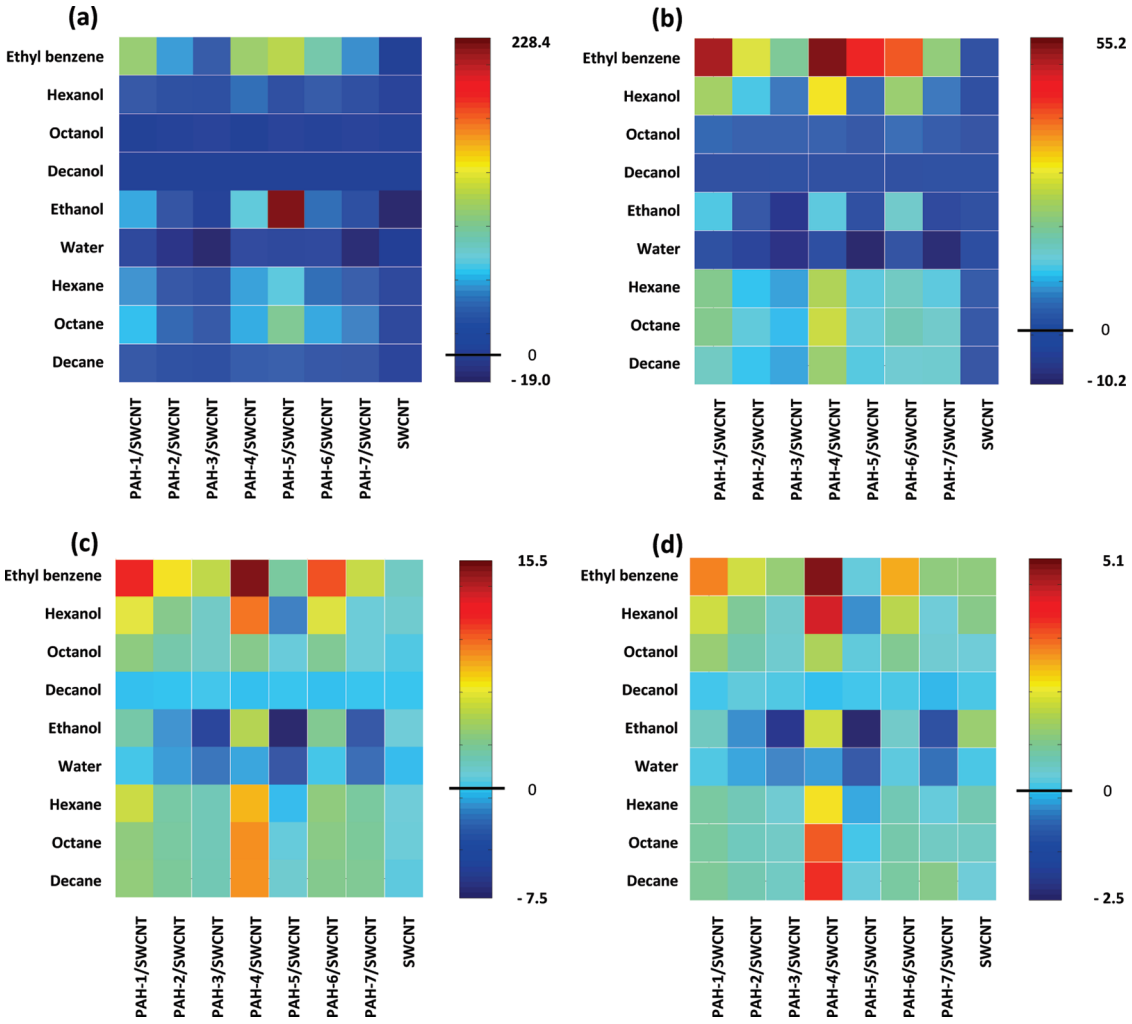

Figure 4. Image plot of S_e values calculated for the VOCs and water analyzed. VOCs concentrations were (a) 1, (b) 0.5, (c) 0.2, and (d) 0.09. The detection capability of the various sensors is represented by the differences in color and intensity of the points.

TABLE 1. Discrimination Accuracy between Polar and Nonpolar VOCs Obtained Using (a) Various Sensors Employed in This Study and (b) Array of Different Sensors

Table 1a

	PAH-1/SWCNTs	PAH-2/SWCNTs	PAH-3/SWCNTs	PAH-4/SWCNTs	PAH-5/SWCNTs	PAH-6/SWCNTs	PAH-7/SWCNTs	SWCNT sensor
nonpolar	37.5%	45.8%	50.0%	50.0%	37.5%	41.7%	50.0%	58.3%
polar	79.2%	77.1%	81.3%	79.2%	77.1%	72.9%	83.3%	62.5%
accuracy	65.3%	66.7%	61.1%	69.4%	63.9%	62.5%	**72.2%**	61.1%

Table 1b

	7PAHs/SWCNTs	6PAHs/SWCNTs	5PAHs/SWCNTs	4PAHs/SWCNTs	3PAHs/SWCNTs	2PAHs/SWCNTs
nonpolar	87.5%	87.5%	79.2%	70.8%	70.8%	58.3%
polar	91.7%	91.7%	93.8%	95.8%	95.8%	95.8%
accuracy	**90.3%**	**90.3%**	88.9%	87.5%	87.5%	83.3%
PAH molecules	all	1,2,3,4,6,7	1,2,4,6,7	1,3,4,7/1,4,6,7	1,4,7	6,7

To investigate the classification between the polar and nonpolar VOC groups for each of the tested sensors, the obtained sensing signals were treated by discriminant factor analysis (DFA);[31] see Methods section for more details. As seen in Table 1, the addition of the PAH improved the discrimination accuracy between the polar and nonpolar VOCs. Among all sensors, the PAH-7/SWCNTs exhibited maximum discrimination accuracy (72.2%) (*cf.* Figure 5a). Nevertheless, an integration of cross-reactive signals from other PAH-SWCNT sensors

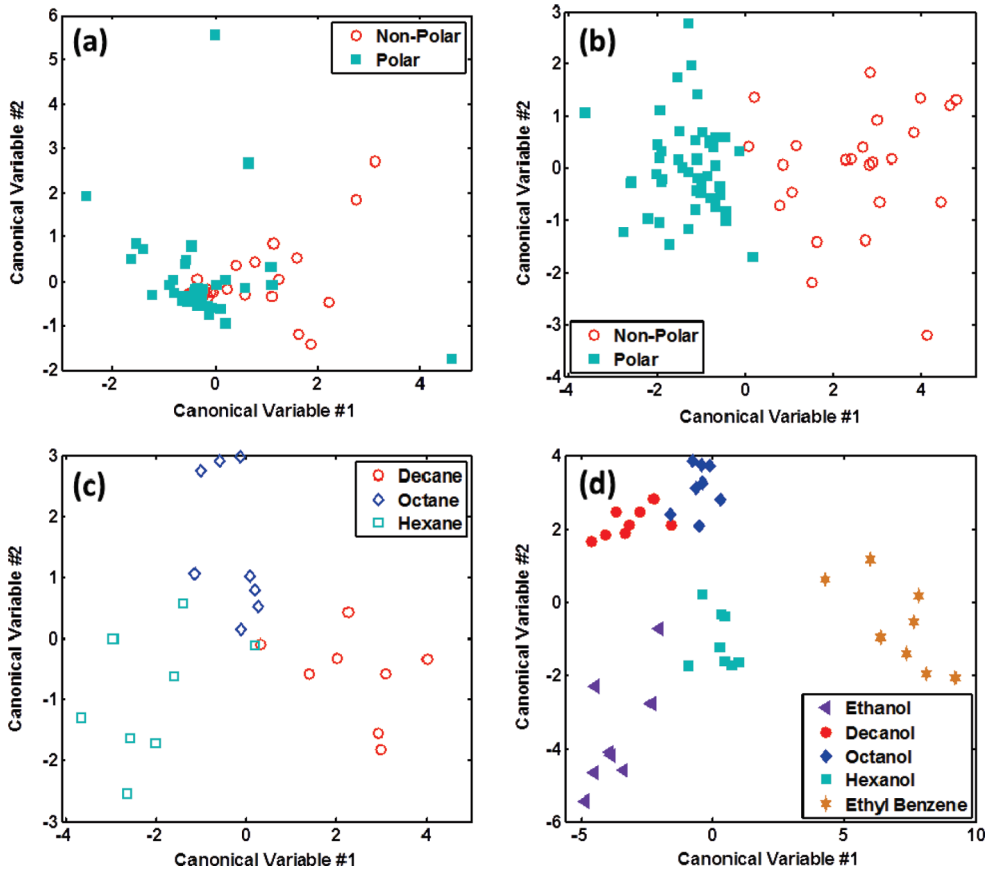

Figure 5. (a) DFA discrimination result between polar and nonpolar VOCs obtained with the PAH-7-functionalized SWCNT sensor; (b) DFA discrimination result between polar and nonpolar VOCs obtained with an array of all PAH-functionalized SWCNT sensors; (c) DFA discrimination result between the nonpolar VOCs obtained with an array of 4 PAH-functionalized SWCNT sensors; (d) DFA discrimination result between the polar VOCs obtained with an array of 5 PAH-functionalized SWCNT sensors.

TABLE 2. Discrimination Accuracy of the Nonpolar VOCs Obtained with an Array of PAH-Functionalized SWCNT Sensors

nonpolar VOCs	4PAHs/SWCNTs	3PAHs/SWCNTs	2PAHs/SWCNTs
decane	87.5%	75%	62.5/62.5%
octane	87.5%	75%	27.5/50.0%
hexane	62.5%	62.5%	87.5/75.0%
accuracy	**79.2%**	70.8%	62.5%
PAH molecules	1,2,3,7	1,3,7	2,4/4,6

TABLE 3. Discrimination Accuracy of the Polar VOCs Obtained with an Array of PAH-Functionalized SWCNT Sensors

polar VOCs	6PAHs/ SWCNTs	5PAHs/ SWCNTs	4PAHs/ SWCNTs	3PAHs/ SWCNTs	2PAHs/ SWCNTs
ethanol	50/37.5%	62.5%	62.5%	37.5%	62.5%
decanol	87.5/75%	87.5%	100.0%	100.0%	100.0%
octanol	75/87.5%	87.5%	87.5%	87.5%	62.5%
hexanol	75/75%	87.5%	75.0%	75.0%	75.0%
ethyl benzene	50/62.5%	75.0%	62.5%	62.5%	75.0%
accuracy	67.5%	**80.0%**	77.5%	72.5%	75.0%
PAH molecules	1,2,3,4,6,7/ 2,3,4,5,6,7	2,3,4,5,6	3,4,5,6	1,6,7	2,3

could increase this accuracy value. The more PAH/SWCNT signals included in this integration, the higher the discrimination accuracy. The best accuracy (90.3%), under $p_a/p_o = 0.04-1$ conditions, was obtained upon integration of six or seven PAH/SWCNT sensors (see Table 1b). Focusing on the nonpolar VOC group, the DFA provided maximum discrimination accuracy (79.2%) between decane, octane, and hexane when an array of four sensors (PAH-1/SWCNT, PAH-2/SWCNT, PAH-3/SWCNT, and PAH-7/SWCNT) was used (see Table 2 and Figure 5c).[32] On the other hand, focusing on the polar VOC group, the DFA provided maximum discrimination accuracy (80%) between ethanol, decanol, octanol, hexanol, and ethyl benzene when an array of five sensors (PAH-2/SWCNT, PAH-3/SWCNT, PAH-4/SWCNT, PAH-5/SWCNT, and PAH-6/SWCNT) was used (see Table 3 and Figure 5d). Subsequently, DFA considerations with all PAH/SWCNT sensors showed a simultaneous discrimination between all tested polar and nonpolar VOCs at various concentration levels. Figure 6 presents the response of the array to $p_a/p_o = 0.04$ at the plot's center. Gradual movement from the plot's center to the periphery indicates a gradual increase of the

p_a/p_o value. In this way, the points closest to the graph boundaries are for $p_a/p_o = 1$ VOC concentration. As seen in Figure 6, the nonpolar VOCs (open symbols) appeared in the second quadrant of the plot (in the northwest direction). Increasing the concentration of the octanol spread the signals east. The decanol formed a very compact cluster close to the approximate center of the graph, most likely because of the extremely weak response of the sensors to this VOC. Increasing the concentrations of the other three polar VOCs (ethanol, hexanol, and ethyl benzene) spread the signal south while exhibiting distinctive pathways in each case. On the other hand, increasing the humidity spread the signal exclusively in the north direction.

Models for predicting the concentration of each VOC were built using the partial least-squares (PLS)[33] method (see Methods for more details). For all cases, a reasonable correlation coefficient (CC) between the real and predicted VOC concentration was obtained (see Table 4).

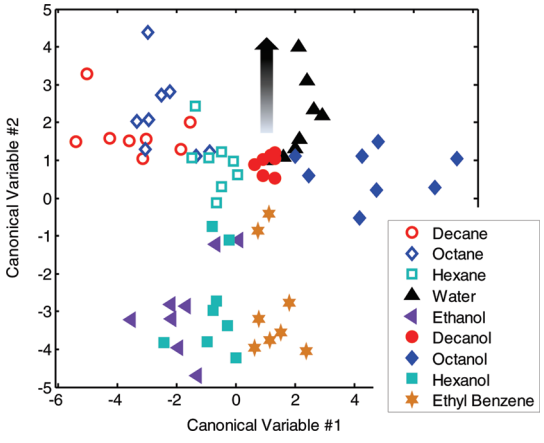

Figure 6. DFA discrimination result between all VOCs obtained with an array of all PAH-functionalized SWCNT sensors. As represented by the black arrow (in the case of water), gradual movement from the plot's center (where $p_a/p_o = 0.04$) to the periphery indicates a gradual increase of the p_a/p_o value. In this way, the points closest to the graph boundaries stand for $p_a/p_o = 1$ VOC concentration.

The results in Table 4 indicate the suitability of PAH/SWCNTs for smart, self-training sensor systems. In particular, as depicted in Table 4, information from different sensors can be exchanged to build a representation of what is happening in the environment.[34] After the model has been built, some needed information can be provided to help the sensor(s) system construct a model for interpreting sensor data readings.

Representative VOCs (octane, ethyl benzene, and ethanol) were measured in an air mixture with a humid background. Figure 3b shows the response of PAH-4/SWCNT and pristine SWCNT sensors toward air with successively increasing concentrations of octane+5% RH, water (80% RH), and octane+80% RH. As could be seen in the figure, the NR of the pristine SWCNTs exhibited positive values upon exposure to octane+5% RH and negative values upon exposure to 80% RH or upon exposure to octane+80% RH. As water

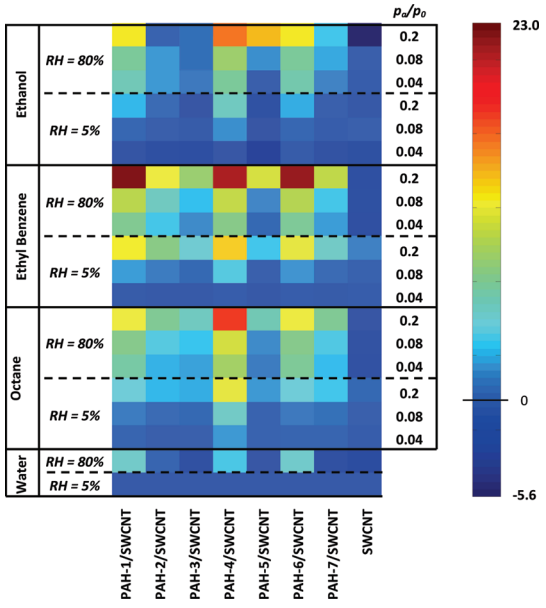

Figure 7. Hot-plot representation of S_e values calculated for different VOC exposures in dry (5%) and highly humid (80% RH) airflow, as well as for exposures to 80% RH airflow.

TABLE 4. Correlation Coefficient between Real and Estimated VOC Concentrations Obtained Using the Various Sensors Employed in This Study[a]

VOC	PAH-1/SWCNTs	PAH-2/SWCNTs	PAH-3/SWCNTs	PAH-4/SWCNTs	PAH-5/SWCNTs	PAH-6/SWCNTs	PAH-7/SWCNTs	SWCNTs
decane	0.9755	0.9765	0.9814	0.9372	**0.9962**	0.9797	0.9815	0.9870
octane	0.9896	0.9767	0.9797	**0.9990**	0.9336	0.9581	0.9730	0.9800
hexane	0.9946	0.9810	0.9772	**0.9998**	0.9553	0.9835	0.9876	0.9877
water	0.8563	0.6665	0.6187	0.7778	0.0998	**0.9564**	0.5682	0.9054
ethanol	**0.9592**	0.9461	0.5619	0.9298	0.9027	0.9406	0.8416	0.9160
decanol	0.7000	0.8450	**0.8678**	0.7421	0.6725	0.2943	−0.2290[b]	0.4565
octanol	0.5387	0.3742	0.3274	**0.8204**	0.3380	0.6277	0.3907	0.3021
hexanol	0.8386	0.9036	0.9670	0.9020	0.9384	0.8680	**0.9841**	0.7120
ethyl benzene	0.9936	0.9605	0.9207	0.9937	0.9841	0.9770	**0.9962**	0.8223

[a] Two replicates per each VOC concentration (*i.e.*, 1, 0.5, 0.2, and 0.09), providing a total number of eight different samples, were used to calculate each correlation coefficient. The most appropriate sensor for predicting the concentration of each particular VOC is clearly evidenced in the table. [b] A negative correlation coefficient indicates a negative linear relationship; *i.e.*, while one variable increases (*e.g.*, the actual concentration), the other decreases (*e.g.*, predicted concentration), and *vice versa*.

TABLE 5. Discrimination Accuracy between Octane, Ethyl Benzene, and Ethanol Measurements Diluted in Highly Humid (80% RH) Carrier Airflow, Using (a) Various Sensors Employed in This Study and (b) Array of Different Sensors

Table 5a

	PAH-1/SWCNT	PAH-2/SWCNT	PAH-3/SWCNT	PAH-4/SWCNT	PAH-5/SWCNT	PAH-6/SWCNT	PAH-7/SWCNT	SWCNT
octane	33.3%	16.7%	0%	33.3%	16.7%	50.0%	0%	16.7%
ethyl benzene	83.3%	83.3%	33.3%	100%	83.3%	83.3%	66.7%	50.0%
ethanol	100%	100%	100%	83.3%	100%	83.3%	100%	100%
accuracy	**72.2%**	66.7%	44.4%	**72.2%**	66.7%	**72.2%**	55.6%	55.6%

Table 5b

	3PAHs/SWCNT	2PAHs/SWCNT
octane	100%	100/100/100
ethyl benzene	100%	100/83.3/83.3
ethanol	100%	83.3/100/100
accuracy	**100%**	94.4%
PAH molecules	1,3,4	1,4/3,4/4,7

molecules behave as electron donors to the SWCNTs, this turn over effect could be explained by the opening of electron channels at high humidity levels (>65%).[35] Coating the SWCNTs with a PAH-4 layer exhibited improved responses, compared to pristine SWCNTs, with positive values for 80% RH, octane+5% RH, and octane+80% RH. A similar observation was noted upon exposure of the PAH-4/SWCNT sensor to ethyl benzene and ethanol. All results were reproducible, within ±9% experimental error, from cycle to cycle and from sample to sample. These observations imply two possible mechanisms: (1) the PAH-4 film coating the SWCNTs acts as a water-selective filter that permits VOC diffusion and adsorption into the SWCNT network but blocks/inhibits the penetration of water molecules through the PAH-4 film (in accordance with the gradual *versus* spike-like resistance change of the PAH-4/SWCNT sensor when exposed to 80% RH and to octane, respectively); or (2) a combination of resistance and an increase in the PAH-4 film, together with an overall lower resistance compared to the SWCNT network, makes the PAH-4 film the dominant sensing element for humidity. Figure 7 presents an image plot of the S_e values calculated from the pristine SWCNT and PAH/SWCNT sensors upon exposure to various VOCs at different concentrations (p_a/p_o = 0.04, 0.08, and 0.2) and background humidity. Each point in these plots is an average of three independent exposures from three duplicated sensors.[25] As seen in the figure, although the incorporation of the PAHs slightly increased the sensitivity to humidity, it substantially improved the sensing signals toward part or all of the tested VOCs, as compared to pristine SWCNTs. The higher the VOC concentration, the higher the detection improvement. In many cases, the higher the relative humidity in the mixture, the higher the improvement as compared to pristine SWCNTs. In some cases, such as for the PAH-5/SWCNT sensor, the sensitivity to the polar VOCs (ethyl benzene and ethanol) increased with the increase in the RH. This is indicated by the enhanced color variation when VOC

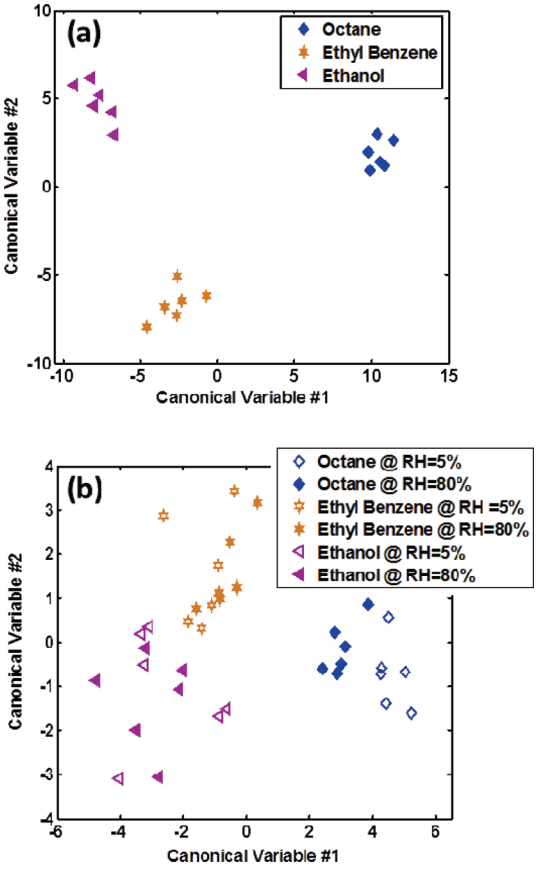

Figure 8. (a) DFA discrimination result between octane, ethyl benzene, and ethanol measurements diluted in highly humid (80% RH) carrier airflow, obtained with an array of 3 PAH-functionalized SWCNT sensors. (b) DFA discrimination result between octane, ethyl benzene, and ethanol measurements diluted in both dry (5% RH) and highly humid (80% RH) carrier airflow, obtained with an array of 4 PAH-functionalized SWCNT sensors. Open symbols represent measurements performed at 5% RH, while filled symbols represent measurements performed at 80% RH.

TABLE 6. Discrimination Accuracy between Octane, Ethyl Benzene, and Ethanol Measurements Diluted in Both Dry (5% RH) and Highly Humid (80% RH) Carrier Airflow, Using (a) Various Sensors Employed in This Study and (b) Array of Different Sensors

Table 6a

	PAH-1/SWCNT	PAH-2/SWCNT	PAH-3/SWCNT	PAH-4/SWCNT	PAH-5/SWCNT	PAH-6/SWCNT	PAH-7/SWCNT	SWCNT
octane	33.3%	33.3%	41.7%	41.7%	33.3%	33.3%	25.0%	8.3%
ethyl benzene	58.3%	41.7%	8.3%	33.3%	33.3%	25.0%	16.7%	16.7%
ethanol	91.7%	83.3%	83.3%	83.3%	100%	75.0%	91.7%	83.3%
accuracy	**61.1%**	52.8%	44.4%	52.8%	55.6%	44.4%	44.4%	36.1%

Table 6b

	6PAHs/SWCNT	5PAHs/SWCNT	4PAHs/SWCNT	3PAHs/SWCNT	2PAHs/SWCNT
octane	100%	100%	100%	100%	100%
ethyl benzene	83.3%	83.3%	83.3%	83.3%	66.7%
ethanol	75.0%	91.7%	91.7%	91.7%	100%
accuracy	86.1%	**91.7%**	**91.7%**	**91.7%**	88.9%
PAH molecules	1,2,4,5,6,7	1,2,4,5,7	2,4,5,6	2,4,6	2,4

TABLE 7. Correlation Coefficient between Real and Estimated VOC Concentrations for the Measurements Performed at 80% RH Obtained Using the Various Sensors Employed in This Study[a]

VOC	PAH-1/SWCNTs	PAH-2/SWCNTs	PAH-3/SWCNTs	PAH-4/SWCNTs	PAH-5/SWCNTs	PAH-6/SWCNTs	PAH-7/SWCNTs	SWCNTs
octane	0.9952	0.9913	0.9418	**0.9990**	0.9852	0.9729	0.9869	0.7849
ethyl benzene	0.9900	0.9675	0.9432	**0.9981**	0.9797	0.9246	0.9760	0.8885
ethanol	0.9942	0.9432	0.7560	**0.9976**	0.9869	0.8281	0.4199	0.9415

[a] Two replicates per each VOC concentration (*i.e.*, 0.2, 0.08, and 0.04), providing a total number of six different samples, were used to calculate each correlation coefficient. The most appropriate sensor for predicting the concentration of each particular VOC is clearly evidenced in the table.

concentrations are increased in a background of 80% RH compared to 5% RH. The classification results based on the S_e feature obtained under 80% RH conditions are summarized in Table 5a. Among all individual sensors, PAH-1/SWCNT or PAH-4/SWCNT or PAH-6/SWCNT exhibited maximum discrimination accuracy (72.2%); see Table 5a and Figure 7 (showing enhanced color variation for these sensors). This discrimination accuracy could be further enhanced by integrating sensing signals from other sensor types. A combination of two or three PAH/SWCNT sensors, under p_a/p_o = 0.04−1, increased the discrimination accuracy to 94.4 or 100%, respectively (see Table 5b and Figure 8). The discrimination power of each sensor, based on the S_e feature, under both VOC+5% RH and VOC+80% RH conditions is summarized in Table 6a. The best accuracy in this case (61.1%) was obtained by the PAH-1/SWCNT sensor. Of special interest, the PAH-5/SWCNT sensor was able to correctly classify ethanol at different concentrations and different humidity levels in the sampled mixtures. This is an important achievement that could serve as the basis for immediate development of reliable alcohol breath analyzers (which currently lack robust accuracy) as well as diagnostic tools for oxidative stress and alcohol-related diseases (*e.g.*, liver disease, hyperlactacidemia, *etc.*).[36]

The discrimination of the VOCs in the 5−80% RH interval reached 91.7% accuracy when data from a combination of various PAH/SWCNT sensors was adopted (see Table 6b). Figure 8b shows the DFA discrimination between octane, ethyl benzene, and ethanol diluted in 5 and 80% RH, as obtained with an array of PAH-2/SWCNT, PAH-4/SWCNT, PAH-5/SWCNT, and PAH-6/SWCNT sensors. As seen in the figure, the selected PAH/SWCNT sensor array was able to reliably discriminate between the different VOCs, irrespective of the humidity level in the sample. A study for understanding the structure−property relationship between the PAH corona, PAH substituent functionality, PAH/SWCNT binding interface, and the VOC chemical nature is underway and will be published elsewhere.

The PLS algorithm revealed an excellent correlation between real and estimated VOC concentrations in a mixture with 80% RH (Table 7). As the table shows, the PAH-4/SWCNT sensor exhibited CC = 0.9990 for octane, CC = 0.9981 for ethyl benzene, and CC = 0.9976 for ethanol. All PAH/SWCNT sensors exhibited higher CC values than the pristine SWCNT sensor in predicting the concentration of octane (nonpolar VOC) and ethyl benzene (weakly polar VOC) in a mixture having 80% RH (see Table 7). For polar molecules, PAH-1/SWCNTs, PAH-4/SWCNT, and PAH-5/SWCNTs exhibited the best CC (>0.9869) values, slightly higher than the CC values obtained by the pristine SWCNT sensor (0.9415). Such results further increase the chances to use these

sensors in self-training systems, such as robots and diagnostic, screening, and/or prevention tools.[34]

SUMMARY AND CONCLUSIONS

We provide extensive and comprehensive evidence that employing PAHs with various aromatic coronae and functional substituents allows reliable discrimination between polar and nonpolar groups and, also, between the different components in each of these VOC groups. In most cases, good discrimination between the VOC and water signals was obtained. A cross-reactive array that is based on PAH/SWCNT sensors and DFA and/or PLS recognition methods exhibited discrimination between various VOCs in mixtures with either 5 or 80% RH. Using appropriate combinations of PAH/SWCNT sensors, the sensitivity and accuracy of the cross-reactive PAH/SWCNT array was tailored according to the detection (or application) of interest. Combining the sensors with the PLS algorithm allowed prediction of VOC concentration in various constant humidity levels. This result is of great importance for the construction of smart, self-learning sensing systems that can work independently under real confounding factors. Using the PAH/SWCNT sensors, it will be possible to exchange information and construct a model of some environmental properties under observation. Such a model can then be used to classify events of interest and take actions on the basis of a high-level representation of the system context. This would allow pervasive information and communication systems using the model to autonomously adapt to highly dynamic and open environments.

Ultimately, the results presented here could lead to the development of a cost-effective, lightweight, low-power, non-invasive tools for the widespread detection of VOCs in real-world applications, including, but not confined to, environmental, security, food, health, or disease diagnosis from breath analysis applications (just to name only a few). A study for understanding the structure–property relationship between the PAH corona, PAH substituent functionality, PAH/SWCNT binding interface, and the VOC chemical nature is underway and will be published elsewhere.

METHODS

Fabrication of Sensors. The sensors were prepared on device quality, degeneratively doped p-type Si(100) wafers capped with a 2 μm thick thermally grown SiO_2 insulating layer. Ten pairs of 4.5 mm wide, interdigitated (ID) electrodes with an interelectrode spacing of 100 μm were formed on the substrates by evaporation of 5 nm/40 nm Ti/Pd layer through a shadow mask. SWCNTs (from ARRY International LTD, Germany; ~30% metallic, ~70% semiconducting, average diameter = 1.5 nm, length = 7 mm) were dispersed in dimethylformamide (DMF, from Sigma Aldrich Ltd., >98% purity) using sonication for 15 min, resulting in a 0.02 wt % dispersion, which was then left for 0.5 h in a 50 mL vial for sedimentation of large aggregates. The resulting homogeneous dispersion above the precipitate was then taken from the vial and further purified by ultracentrifugation for 25 min. The purification procedure was performed twice to ensure that the majority of the aggregates and impurities were removed. Electrically continuous random network of SWCNTs were formed by drop-casting the SWCNT dispersion onto the preprepared ID electrodes (see Figure 1a). After the deposition, the devices were slowly dried overnight under ambient conditions to enhance the self-assembly of the SWCNTs and to evaporate the solvent. The procedure was repeated until a resistance of 100 KΩ to 10 MΩ was obtained. As a reference, devices that included pristine PAH only exhibited a baseline resistance of 1–2 TΩ.

The SWCNT layers were then coated with seven PAH compounds having different aromatic coronae and side groups (see Figure 2). The synthesis of PAH-1,[28] PAH-2,[29] and PAH-7[30] has been described in previous reports, whereas the synthesis of PAHs 3–6 will be reported elsewhere. These PAH derivatives contain hydrophobic mesogens that are terminated with different alkyl chains and functional substituents, such as alcohol (for PAH-6), ester (for PAH-2 and PAH-3), carboxylic acid (for PAH-4 and PAH-5), *etc*. PAH-1, PAH-2, and PAH-6 contain a PAH aromatic core (with a carbon number of 42), while PAH-3, PAH-4, and PAH-5 have a semi-triangle-shaped aromatic core (with a carbon number of 48) and PAH-7 possesses a triangle-shaped core (with a carbon number of 50). These molecules are able to self-assemble into long molecular stacks with a large, electron-rich, semiconducting core, which guarantees good charge carrier transport along the molecular stacking direction and a relatively insulating periphery.[28–30,37] Furthermore, the nanometer thick PAH columns can easily form 3D, micrometer-sized, sponge-like structures with a high surface-to-volume ratio.[18] In this work, we have examined the affinity of PAH layers, so-called adsorption layers, to a variety of VOCs and mixtures of VOC and water vapor.

Nearly continuous, polycrystalline PAH layers were formed on top of the SWCNTs by drop-casting 10 μL of 10^{-3} M solution in toluene of either PAH-1, PAH-2, PAH-3, PAH-6, and PAH-7 or 10 μL of 10^{-3} M solution in tetrahydrofuran (THF) of either PAH-5 or PAH-6 (see Figure 1b for a representative example). After the fabrication, the devices were slowly dried under ambient conditions for 2–5 h to enhance the self-assembly of these PAH molecules and to evaporate the residual solvent. The deposition process was repeated until the molecules formed nearly continuous layers that completely cover the supporting and conductive SWCNT layer, as verified by scanning electron microscopy (see Figure 1b) and resistance measurements. The baseline resistance of the PAH/SWCNT sensors generally ranged between ~90 kΩ and a few MΩ, except for the PAH-4/SWCNT sensor, whose baseline resistance was ~5 kΩ.

Characterization of Sensors. Eight representative VOCs diluted in synthetic airflow containing ~5 or ~80% relative humidity (RH) have been analyzed in this study. Most importantly, water is a polar compound (dipole moment = 1.85 D) that usually screens the VOC signals in mixtures of VOCs and water.[4,12] For the current study, DI water (18.2 MΩ·cm) was supplied by a commercial water purification system (Easy Pure II). Hexane, octane, and decane (all obtained from Sigma Aldrich Ltd.) were used as representative examples for nonpolar alkane hydrocarbons (dipole moment = 0 D). Ethyl benzene (Sigma Aldrich Ltd.) was used as a representative example for aromatic VOCs (dipole moment = 0.4 D). Hexanol (dipole moment = 1.42 D), octanol (dipole moment = 2 D), decanol (dipole moment = 1.68 D), and ethanol (dipole moment = 1.684 D), all received from Sigma Aldrich Ltd., were used as representative cases for polar VOCs.

The sensors were tested electrically during exposure to the VOCs of interest in an automated, computer-controlled flow system. This system is capable of regulating the VOC concentration *via* their vapor pressure. For this study, the sensors were investigated under a range of concentrations,

from $p_a/p_o = 0.04$ to $p_a/p_o = 1$, where p_a is the partial pressure of the VOC and p_o is the saturated vapor pressure at 21 °C. The response of the pristine SWCNT and the PAH/SWCNT sensors was tested simultaneously, in the same exposure chamber, using an Agilent multifunction switch 34980. A Stanford Research System SR830 DSP lock-in amplifier controlled by an IEEE 488 bus was used to supply the AC voltage signal (0.2 V at 1 kHz) and to measure the corresponding current (<10 μA in the studied devices). This setup enables measuring normalized changes in conductance as small as 0.01%. Sensing experiments were performed continuously, using subsequent exposure cycles, each cycle consisting of three main steps: (i) exposure to synthetic airflow with 5% RH for 10 min; (ii) exposure to the VOC of interest (at a given concentration), with or without humidity background, for 10 min; and (iii) purging the chamber/sensors by a synthetic airflow with 5% RH for 10 min. In order to acquire reliable data, each measurement was repeated at least twice on two duplicates that were prepared from different batches.

Data Analysis. Three parameters were extracted from each sensor response: (i) the normalized change in sensor resistance at half of the time after VOC exposure (S_h); (ii) the corresponding value at the end of the VOC exposure (S_e); and (iii) the area under the response curve (S_a). An advanced discrimination between the various VOCs was carried out by employing a discriminant factor analysis (DFA) algorithm.[31] DFA is a supervised linear method that is supplied with the classification information regarding every measurement in the training set. DFA finds new orthogonal axes (canonical variables) as a linear combination of the input variables, computing these factors to minimize the variance within each class and maximize the variance between classes. The accuracy of VOC classification is calculated employing a leave-one-out cross-validation method. Given n measurements, DFA is computed n times using $n - 1$ training vectors. The vector left out during the training phase (*i.e.*, validation vector that is unseen by the DFA method during the training phase, thus completely new for the DFA model built) is then projected onto the DFA model built, which has produced a classification result. The classification accuracy is estimated as the averaged performance over the n tests.

A linear multivariate statistical algorithm, specifically partial least-squares (PLS),[33] was used to build predictive models for estimating VOC concentrations. PLS is a multivariate calibration method that attempts to find factors (*i.e.*, latent variables), which capture as much variance as possible in the predictor block (response matrix), under the constraint of being correlated with the predicted block (concentration matrix). The prediction of the VOC concentration was evaluated using a leave-one-out cross-validation method. Thus, for each VOC, a model was built n times using $n - 1$ measurements, and the remaining one has been used for testing.

Acknowledgment. We acknowledge the financial support from the Marie Curie Excellence Grant of the FP6 and from the FP7's ERC grant under DIAG-CANCER (Grant Agreement No. 256639) and G. Konvalina for constructive comments on the manuscript. H.H. is a Knight of the Order of Academic Palms.

REFERENCES AND NOTES

1. Tisch, U.; Haick, H. Nanomaterials for Cross-Reactive Sensor Arrays. *MRS Bull.* **2010**, *35*, 797.
2. Kara, P.; Escosura-Muñiz, A.; Costa, M. M.; Guix, M.; Ozsoz, M.; Merkoçi, A. Aptamers Based Electrochemical Biosensor for Protein Detection Using Carbon Nanotubes Platforms. *Biosens. Bioelectron.* **2010**, *26*, 1715–1718.
3. Sokolov, A. N.; Roberts, M. E.; Bao, Z. Fabrication of Low Cost Electronic Biosensors. *Mater. Today* **2009**, *12*, 12–20.
4. Roeck, F.; Barsan, N.; Weimar, U. Electronic Nose: Current Status and Future Trends. *Chem. Rev.* **2008**, *108*, 705–725.
5. Kauffman, D. R.; Star, A. Carbon Nanotube Gas and Vapor Sensors. *Angew. Chem., Int. Ed.* **2008**, *47*, 6550–6570.
6. Albert, K. J.; Lewis, N. S.; Schauer, C. L.; Sotzing, G. A.; Stitzel, S. E.; Vaid, T. P.; Walt, D. R. Cross-Reactive Chemical Sensor Arrays. *Chem. Rev.* **2000**, *100*, 2595–2626.
7. Liu, Z.; Tian, J.; Guo, Z.; Ren, D.-M.; Du, F.; Zheng, J.; Chen, Y. Enhanced Optical Limiting Effects in Porphyrin-Covalently Functionalized Single-Walled Carbon Nanotubes (p NA). *Adv. Mater.* **2008**, *20*, 511–515.
8. Persaud, K.; Dodd, G. Analysis of Discrimination Mechanisms in the Mammalian Olfactory System Using a Model Nose. *Nature* **1982**, *299*, 352–355.
9. Wang, D. K. W.; Austin, C. C. Determination of Complex Mixtures of Volatile Organic Compounds in Ambient Air: An Overview. *Anal. Bioanal. Chem.* **2006**, *386*, 1089–1098.
10. Peng, G.; Tisch, U.; Adams, U.; Hakim, M.; Shehada, N.; Broza, Y. Y.; Billan, S.; Abdah-Bortnyak, R.; Kuten, A.; Haick, H. Diagnosing Lung Cancer in Exhaled Breath Using Gold Nanoparticles. *Nat. Nanotechnol.* **2009**, *4*, 669–673.
11. Peng, G.; Tisch, U.; Haick, H. Detection of Nonpolar Molecules by Means of Carrier Scattering in Random Networks of Carbon Nanotubes: Toward Diagnosis of Diseases *via* Breath Samples. *Nano Lett.* **2009**, *9*, 1362–1368.
12. Peng, G.; Trock, E.; Haick, H. Detecting Simulated Patterns of Lung Cancer Biomarkers by Random Network of Single-Walled Carbon Nanotubes Coated with Non-polymeric Organic Materials. *Nano Lett.* **2008**, *8*, 3631–3635.
13. Haick, H.; Hakim, M.; Patrascu, M.; Levenberg, C.; Shehada, N.; Nakhoul, F.; Abassi, Z. Sniffing Chronic Renal Failure in Rat Model by an Array of Random Networks of Single-Walled Carbon Nanotubes. *ACS Nano* **2009**, *3*, 1258–66.
14. Sysoev, V. V.; Button, B. K.; Wepsiec, K.; Dmitriev, S.; Kolmakov, A. Toward the Nanoscopic "Electronic Nose": Hydrogen *vs* Carbon Monoxide Discrimination with An array of Individual Metal Oxide Nano- and Mesowire Sensors. *Nano Lett.* **2006**, *6*, 1584–1588.
15. Rusling, J. F.; Kumar, C. V.; Gutkind, J. S.; Patel, V. Measurement of Biomarker Proteins for Point-of-Care Early Detection and Monitoring of Cancer. *Analyst* **2010**, *135*, 2496–2511.
16. Liu, S.; Mannsfeld, S. C. B.; LeMieux, M. C.; Lee, H. W.; Bao, Z. Organic Semiconductor–Carbon Nanotube Bundle Bilayer Field Effect Transistors with Enhanced Mobilities and High On/Off Ratios. *Appl. Phys. Lett.* **2008**, *92*, 053306.
17. Snow, E. S.; Perkins, F. K.; Houser, E. J.; Badescu, S. C.; Reinecke, T. L. Chemical Detection with a Single-Walled Carbon Nanotube Capacitor. *Science* **2005**, *307*, 1942–1945.
18. Zilberman, Y.; Tisch, U.; Pisula, W.; Feng, X.; Müllen, K.; Haick, H. Sponge-like Structures of Hexa-*peri*-Hexabenzocoronenes Derivatives Enhances the Sensitivity of Chemiresistive Carbon Nanotubes to Nonpolar Volatile Organic Compounds. *Langmuir* **2009**, *25*, 5411–5416.
19. Zilberman, Y.; Tisch, U.; Shuster, G.; Pisula, W.; Feng, X.; Müllen, K.; Haick, H. Carbon Nanotube/Hexa-*peri*-Hexabenzocoronene Bilayers for Discrimination between Nonpolar Volatile Organic Compounds of Cancer and Humid Atmospheres. *Adv. Mater.* **2010**, *22*, 4317–4320.
20. Kastler, M.; Pisula, W.; Wasserfallen, D.; Pakula, T.; Müllen, K. Influence of Alkyl Substituents on the Solution- and Surface-Organization of Hexa-*peri*-Hexabenzocoronenes. *J. Am. Chem. Soc.* **2005**, *127*, 4286–4296.
21. Wu, J.; Pisula, W.; Müllen, K. Graphenes as Potential Material for Electronics. *Chem. Rev.* **2007**, *107*, 718–747.
22. Conceptually, hydrophobic organic monomers, such as hexadecylbenzene or related derivatives, could be utilized for sensing lung cancer VOCs in high humidity atmospheres. Nevertheless, a lack of tailor-made organization features and/or deliberate electrical properties makes them inferior, as compared to the HBC derivatives.
23. Fuhrer, M. S.; Nygard, J.; Shih, L.; Forero, M.; Yoon, Y. G.; Mazzoni, M. S. C.; Choi, H. J.; Ihm, J.; Louie, S. G.; Zettl, A.; *et al.* Crossed Nanotube Junctions. *Science* **2000**, *288*, 494–497.
24. Wang, B.; Ma, Y.; Li, N.; Wu, Y.; Li, F.; Chen, Y. Facile and Scalable Fabrication of Well-Aligned and Closely Packed Single-Walled Carbon Nanotube Films on Various Substrates. *Adv. Mater.* **2010**, *22*, 3067–3070.
25. Considering the S_h or S_a values, instead of the S_e ones, provided similar observations.
26. Dovgolevsky, E.; Tisch, U.; Haick, H. Chemically Sensitive Resistors Based on Monolayer-Capped Cubic Nanoparticles:

Towards Configurable Nanoporous Sensors. *Small* **2009**, *5*, 1158–1161.
27. Dovgolevsky, E.; Konvalina, G.; U., T.; Haick, H. Monolayer-Capped Cubic Platinum Nanoparticles for Sensing Non-polar Analytes in Highly Humid Atmospheres. *J. Phys. Chem. C* **2010**, *114*, 14042–14049.
28. Feng, X. L.; Pisula, W.; Kudernac, T.; Wu, D. Q.; Zhi, L. J.; De Feyter, S.; Müllen, K. Controlled Self-Assembly of C3-Symmetric Hexa-*peri*-Hexabenzocoronenes with Alternating Hydrophilic and Hydrophobic Substituents in Solution, in the Bulk, and on a Surface. *J. Am. Chem. Soc.* **2009**, *131*, 4439–4448.
29. Feng, X. L.; Pisula, W.; Zhi, L. J.; Takase, M.; Müllen, K. Controlling the Columnar Orientation of C3-Symmetric "Superbenzenes" through Alternating Polar/Apolar Substitutents. *Angew. Chem., Int. Ed.* **2008**, *47*, 1703–1706.
30. Feng, X. L.; Liu, M. Y.; Pisula, W.; Takase, M.; Li, J. L.; Müllen, K. Supramolecular Organization and Photovoltaics of Triangle-Shaped Discotic Graphenes with Swallow-Tailed Alkyl Substituents. *Adv. Mater.* **2008**, *14*, 2684–2689.
31. Brereton, R. G. *Chemometrics, Application of Mathematics and Statistics to Laboratory Systems*; Ellis Horwood: Chichester, UK, 1990.
32. The number of sensors in the array should be kept low in order to avoid the overfitting during the training phase. The number of input features for DFA should not be higher than the half of the total number of measurements available.
33. Geladi, P.; Kowalski, B. R. Partial Least Squares Regression—A Tutorial. *Anal. Chim. Acta* **1986**, *185*, 1–17.
34. Zaknich, A. *Principles of Adaptive Filters and Self-Learning Systems*; LE-TEX Jelonek, Schmidt&Vöckler GbR: Leipzig, Germany, 2005.
35. Na, P. S.; Kim, H.; So, H. M.; Kong, K. J.; Chang, H.; Ryu, B. H.; Choi, Y.; Lee, J. O.; Kim, B. K.; Kim, J. J.; *et al.* Investigation of the Humidity Effect on the Electrical Properties of Single-Walled Carbon Nanotube Transistors. *Appl. Phys. Lett.* **2005**, *87*, 093101.
36. Zima, T.; Fialová, L.; Mestek, O.; Janebová, M.; Crkovská, J.; Malbohan, I.; Stípek, S.; Mikulíková, L.; Popov, P. Oxidative Stress, Metabolism of Ethanol and Alcohol-Related Diseases. *J. Biomed. Sci.* **2001**, *8*, 59–70.
37. Feng, X. L.; Marcon, V.; Pisula, W.; Hansen, M. R.; Kirkpatrick, J.; Andrienko, D.; Kremer, K.; Müllen, K. Towards High Charge-Carrier Mobilities by Rational Design of the Shape and Periphery of Discotics. *Nat. Mater.* **2009**, *8*, 421–426.